telecom

MDPI

Article

Polar-Coded Differential/Quadrature Chaos Shift Keying Communication Systems for Underwater Acoustic Channels

Ali Jaber Al-Askery [1,*,†], Fadhil Sahib Hasan [2,†] and Yaser Atta Yassin [1,†]

[1] Department of Automation and Control Engineering Techniques, Electrical Engineering Technical College, Middle Technical University, Baghdad 32001, Iraq; yasser.atta76@mtu.edu.iq
[2] Electrical Engineering Department, College of Engineering, Mustansiriyah University, Baghdad 10052, Iraq; fadel_sahib@uomustansiriyah.edu.iq
* Correspondence: a.alaskery@mtu.edu.iq; Tel.: +964-7817569229
† These authors contributed equally to this work.

Abstract: The underwater acoustic (UWA) channel causes large propagation delays and reduces the bit error rate (BER) of wireless communication systems. The t-distribution is the optimal distribution to perform UWA noise. In this study, polar-coded differential chaos shift keying (DCSK) and quadrature chaos shift keying (QCSK) communication with UWA noise are considered. First, we have proposed a PDF for the UWA noise channel, and based on this PDF, the theoretical BER is derived. Second, polar coding's performance is determined to demonstrate the improvement in the BER performance compared to the uncoded UWA system by means of Monte Carlo simulations. The experimental results prove that the nearest model that is applicable to the UWA channel is a t-distribution with five and six degrees of freedom. The BER formulas of the proposed systems are derived and compared with the simulation results. The results confirm the performance improvement of the polar-coded chaotic modulation systems over uncoded systems in UWA channels.

Keywords: DCSK; QCSK; underwater acoustic; polar-coded systems

check for updates

Citation: Al-Askery, A.; Hasan, F.S.; Yassin, Y.A. Polar-Coded Differential/Quadrature Chaos Shift Keying Communication Systems for Underwater Acoustic Channels. *Telecom* **2024**, *5*, 476–486. https://doi.org/10.3390/telecom5020024

Academic Editor: Mario E. Rivero-Angeles

Received: 11 May 2024
Revised: 30 May 2024
Accepted: 12 June 2024
Published: 18 June 2024

Copyright: © 2024 by the authors. Licensee MDPI, Basel, Switzerland. This article is an open access article distributed under the terms and conditions of the Creative Commons Attribution (CC BY) license (https://creativecommons.org/licenses/by/4.0/).

1. Introduction

Due to the applications of underwater acoustic (UWA) channels in both the military and civilian domains, studying their characteristics and performance is immensely important [1]. UWA channels are characterized by severe multipath interference, high Doppler shifts, strong fading, low data rates, and a constrained bandwidth [2–4]. The probability density function (PDF) of this channel has a broad tail with impulsive behavior which differs from the Gaussian PDF, which makes the t-distribution more convenient to model this channel [5–8].

Deep learning and modulation techniques with channel coding have been investigated widely to improve the bit error rate (BER) in these channels. A UWA statistical communication channel has been proposed in [9], in which small-scale and large-scale effects of random local displacements were discussed. Large-scale gain and micro-multipath components are included in the model, which produce a complex Gaussian distortion. An efficient computational model for numerical channel simulation was developed through analytical evaluation of the properties of time correlation and frequency correlation. Bessel-type functions describe additional variation from surface motion and displacements. An appropriate model for the total energy, or gain, averaged over small scales is a log-normal distribution. The accuracy of the model in representing the distribution of transmission loss and short-term path gains has been confirmed through validation using actual data from experiments. Logarithmic loss has been used to describe large-scale transmission loss.

A new chaotic spread spectrum acoustic communication technique was presented in [10], using a hybrid dynamical system's chaotic signal as a spread spectrum sequence.

Multiple propagation and noise have been lessened through the application of a corresponding chaotic matched filter. This technique removed the requirement for intricate channel modulation–demodulation and equalization technologies, in contrast to conventional acoustic communication. The suggested approach achieved a lower BER than some of the other methods that are currently in use, according to the simulation results.

Walsh code's orthogonal characteristic was used to combine chaotic reference chips and information-bearing chips in the same time/frequency unit, as shown in [11]. A cyclic-shift interleaver was employed to take advantage of frequency diversity in the chips. The system's BER was analyzed and validated under Gaussian channels and multipath Rayleigh fading channels through simulation. The proposed system's spectral efficiency was compared with other chaos-based communication systems. The study also evaluated BER performance under UWA channels, comparing it with traditional MC direct sequence spread spectrums (SSs) and orthogonal frequency-division multiplexing (OFDM)-based MC-differential chaos shift keying (DCSK) systems. The simulation results confirmed the system's strength under time-varying UWA channels.

A brief manual for simulating UWA channels has been provided in [12], emphasizing network modeling. A well-balanced method was presented that combines the ease of automated modeling with systems such as the World Ocean Simulation System (WOSS) with the adaptability of low-level channel modeling through beam tracing. A MATLAB simulation code that interfaces with BELLHOP to produce channel data for underwater acoustic network (UAN) simulations has been included in the tutorial. The research included a case study for each of the two ways to incorporate these data into network simulations: (1) directly import them as a look-up table and (2) use them to build a statistical channel model. The paper's main goal was to provide UAN protocol researchers with a useful modeling tool and learning resource. The statistical channel modeling approach's insights highlight its potential as a reliable tool for upcoming UAN research.

A study on underwater wireless sensor networks (UWSNs) was conducted in [13] by simulating the channel capacity in accordance with the water temperature and salinity. The result showed the effects of different criteria such as the weather, the environment and the temperature on the channel characteristics. An algorithm that utilizes machine learning with quality prediction was proposed in [14] for UWA networks. A logistic regression (LR) algorithm was used to predict the BER between the transmitter and the receiver. This prediction involves the signal-to-noise ratio (SNR), temperature and wind speed, in addition to several environmental factors. As a result, the consumed energy was reduced and the method was validated by means of practical experiments in Furong Lake.

An algorithm that utilizes OFDM systems in UWA channels with joint channel estimation and impulsive noise mitigation has been proposed in [15], combining sparse Bayesian learning with Kalman filtering. The proposed algorithm integrates the subcarriers using the SBL algorithm and Kalman filter to jointly estimate time-varying channels, detect data and enhance the efficiency. To validate this algorithm, experiments were performed in Swan River in Australia to collect data, and the results showed improvement in terms of the BER and frame error rate.

To achieve a higher data rate and an improved BER performance, a system has been introduced in [16] that utilizes mapping additional bits to the cyclic shift length of superimposed sequences in in-phase/quadrature branches. Through simulation and field testing, the system's effectiveness in time-varying UWA transmission environments was demonstrated. The system was also theoretically analyzed for the BER over an additive white Gaussian noise (AWGN) channel.

In this paper, an investigation into polar-coded DCSK communication systems for UWA channels is performed, assuming a t-distribution with five and six degrees of freedom. This investigation started by proposing a PDF for the noise distribution and verifying its accuracy by means of a goodness-of-fit method; then, the result is used to derive a theoretical BER and is compared to that from the Monte Carlo simulation. Then, the polar-coded system is investigated to show the improvement to the BER compared to the

uncoded performance. This work is organized as follows: in Section 3, the channel model for the UWA is presented, Section 2 presents the polar code and how it is adopted in the proposed system, Section 4 demonstrates the DCSK and QCSK system models for UWA, Section 5 contains the BER analysis, Section 6 presents the simulation and results, Section 7 discusses the results, and this paper is concluded in Section 8.

2. Polar Code

An error control code with successive cancellation that approaches capacity has been implemented, based on [17]. Two distinct results appear, noiseless channels and nearly fully noisy channels, as the codeword length M approaches infinity with M polarized channels. Information bits are allocated across channels with pure noise during the encoding process, while frozen bits are transmitted through noiseless channels. The information vector $x_1^M = (x_1, x_2, \ldots, x_M)$ represents J-bit information x_A and the remaining bits are frozen and denoted as x_A^c, with $R = \frac{J}{M}$ as the coding rate. The codeword has the form:

$$x_1^M = x_1^M G_M = x_1^M B_M F_2^{\otimes m} \tag{1}$$

where G_M, B_M and $F_2^{\otimes m}$ represent the generator matrix, the bit reversal permutation matrix and the mth Kronecker power of F_2, respectively. F_2 represents the kernel matrix, that is:

$$F_2 = \begin{bmatrix} 1 & 0 \\ 1 & 1 \end{bmatrix} \tag{2}$$

At the receiver, the successive cancellation (SC) decoder generates $\hat{x}_1^M$ as an estimated x_1^M by observing (y_1^M, x_{A^c}); the likelihood ratio (LR) $L_M^{(i)}(y_1^M, \hat{x}_1^{i-1})$ can be calculated from

$$L_M^{(i)}\left(y_1^M, \hat{x}_1^{i-1}\right) = \frac{W_M^{(i)}\left(y_1^M, \hat{x}_1^{i-1} \mid 0\right)}{W_M^{(i)}\left(y_1^M, \hat{x}_1^{i-1} \mid 1\right)} \tag{3}$$

where $W_M^{(i)}\left(y_1^M, \hat{x}_1^{i-1} \mid \gamma\right)$ is the probability of noise that γ is 0 or 1. The decision is

$$\hat{x}_i = \begin{cases} x_i, & i \in A^c \\ h_i\left(y_1^M, \hat{x}_1^{i-1}\right), & i \in A \end{cases} \quad (i = 1, 2, 3, \ldots, M) \tag{4}$$

and

$$h_i\left(y_1^M, \hat{x}_1^{i-1}\right) = \begin{cases} 0, & L_M^{(i)}\left(y_1^M, \hat{x}_1^{i-1}\right) \geq 1 \\ 1, & \text{otherwise} \end{cases} \tag{5}$$

where h_i represents the decision functions that are sent to all succeeding decision elements (DEs). LR calculation based on recursive formulas is given as:

$$L_M^{(2i-1)}\left(y_1^M, \hat{x}_1^{2i-2}\right) = f\left(L_{M/2}^{(i)}\left(y_1^{M/2}, \hat{x}_{1,o}^{2i-2} \oplus \hat{x}_{1,e}^{2i-2}\right), L_{M/2}^{(i)}\left(y_{M/2+1}^M, \hat{x}_{1,e}^{2i-2}\right)\right) \tag{6}$$

$$L_M^{(2i)}\left(y_1^M, \hat{x}_1^{2i-1}\right) = g\left(L_{M/2}^{(i)}\left(y_1^{M/2}, \hat{x}_{1,o}^{2i-2} \oplus \hat{x}_{1,e}^{2i-2}\right), L_{M/2}^{(i)}\left(y_{M/2+1}^M, \hat{x}_{1,e}^{2i-2}\right), \hat{x}_{2i-1}\right) \tag{7}$$

$$f(a, b) = \frac{1 + ab}{a + b} \tag{8}$$

$$g(a, b, \hat{x}_{sum}) = a^{1-2\hat{x}_{sum}} b \tag{9}$$

a, b and $\hat{x}_{sum}$ are defined as follows

$$a = L_{M/2}^{(i)}(y_1^{M/2}, \hat{x}_{1,0}^{2i-2} \oplus \hat{x}_{1,e}^{2i-2}) \tag{10}$$

$$b = L^{(i)}_{M/2}(y^{M}_{M/2+1}, \hat{x}^{2i-2}_{1,e}) \tag{11}$$

$$\hat{x}_{sum} = \hat{x}_{2i-1} \tag{12}$$

3. UWA Channel and Noise Models

In this section, the channel models for the UWA system represented by the noise effect will be demonstrated using MATLAB R2023b simulations to show the matching characteristics. UWA noise modeling is performed based on [4] utilizing a MATLAB fitting tool, while the noise is measured at a depth of 4 m–12 m. The histogram function of MATLAB is utilized on the noise model at the receiver and compared with different PDFs with a t-distribution, that is [4],

$$f_r(x,d) = \frac{\Gamma\left[\frac{d+1}{2}\right]}{\sigma\sqrt{\pi(d-2)}\Gamma\left(\frac{d}{2}\right)}\left(1+\frac{x^2}{\sigma^2(d-2)}\right)^{-\frac{d+1}{2}} \tag{13}$$

where $\Gamma(\cdot)$ is the Gamma function, σ is the standard deviation, d is the degree of freedom for the t-distribution function and x is the random variable. The nearest model that is applicable to this model is a t-distribution with five and six degrees of freedom, that is:

$$\left.\begin{aligned} f_r(x,5) &= \tfrac{0.49}{\sigma}\left(1+\tfrac{(x+\mu)^2}{3\sigma^2}\right)^{-3} \\ f_r(x,6) &= \tfrac{0.46875}{\sigma}\left(1+\tfrac{(x+\mu)^2}{4\sigma^2}\right)^{-3.5} \end{aligned}\right\} \tag{14}$$

The histogram plot of the noise model vs. Equation (14) is shown in Figure 1, which demonstrates the close match between the two plots. In addition, to verify the close match between these plots, a Kolmogorov–Smirnov (KS) goodness-of-fit test [18–20] is used at a significance level of 5%. The test result was 0, showing that the two samples are close and cannot be rejected, especially at a degree of freedom of six.

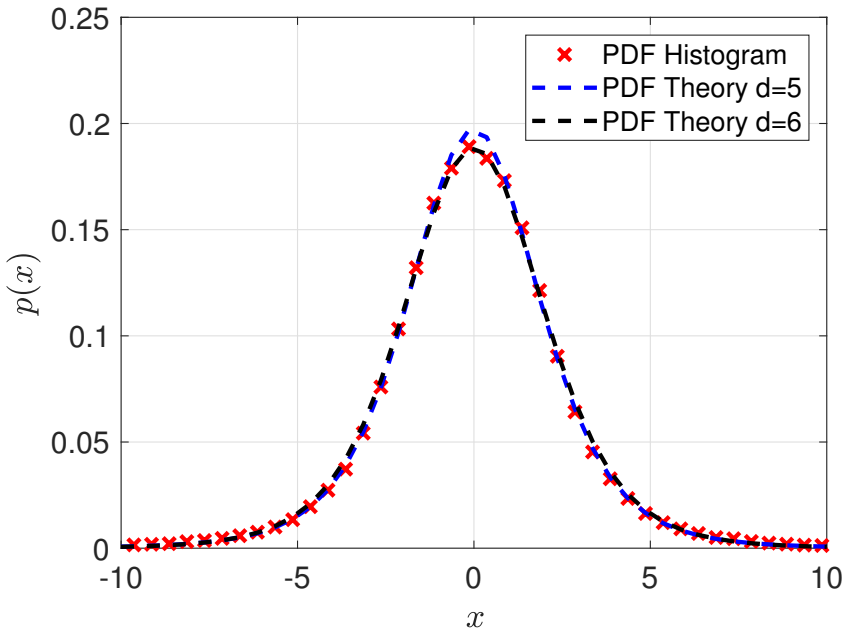


Figure 1. Comparing the histogram of the noise model with the t−distribution at five and six degrees of freedom.

4. DCSK and QCSK Communication Systems for UWA

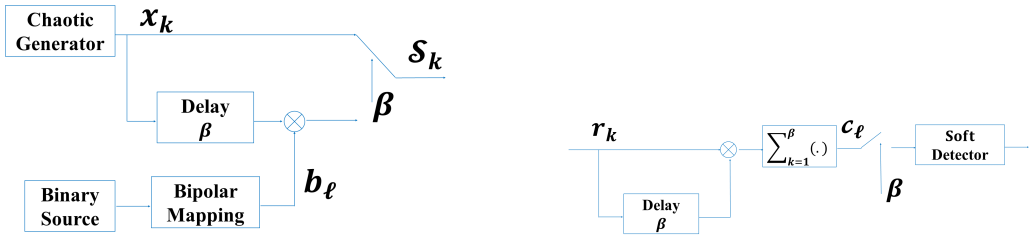
Figure 2 shows the transmitter and receiver block of a DCSK system. Firstly, the lth input datum is mapped to symbol $b_l \in 1$; then, the DCSK transmitter signal S_k for the first input datum is given by [21]:

$$S_k = \begin{cases} x_k & k = 1.\cdots,\beta \\ b_1 x_{k-\beta} & k = \beta+1,\cdots,2\beta \end{cases} \tag{15}$$

where 2β represents the spreading factor. At the receiver, the output of the correlator represents the decision variable of the lth bit, c_l, which is expressed as:

$$c_l = \sum_{k=1}^{\beta} r_k \cdot r_{k+\beta} \tag{16}$$

where r_k is the received sequence. Here, we do not need to pass the decision variable through thresholding since the output of the correlator is directly connected to the polar decoder.



(**a**) Transmitter (**b**) Receiver

Figure 2. Proposed DCSK transmitter and receiver system.

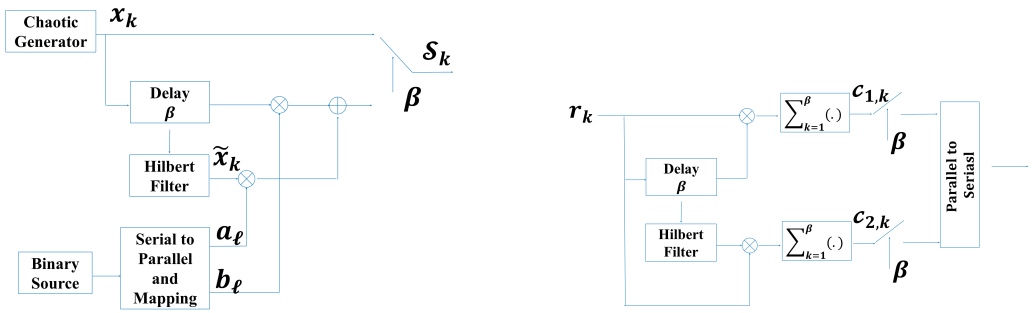
Figure 3 shows the transmitter and receiver block of the QCSK system. Firstly, the lth parallel two symbols $a_l, b_l \in 1$ are multiplied by the reference chaotic sequence and Hilbert transform of the reference chaotic sequence, respectively. After that, the two multiplied sequences are summed and modulated using the same scenario for the DCSK system. The QCSK transmitter signal S_k for the first two input data is given by [22]:

$$S_k = \begin{cases} x_k, & k = 1,\cdots,\beta \\ \frac{1}{\sqrt{2}}(a_1 x_{k-\beta} + b_1 \tilde{x}_{k-\beta}), & k = \beta+1,\cdots,2\beta \end{cases} \tag{17}$$

where $\tilde{x}_k$ is the Hilbert transform of the x_k signal. At the receiver, the two outputs of the correlators represent the decision variables $c_{1,l}$ and $c_{2,l}$, which are expressed as:

$$\begin{aligned} c_{1,l} &= \sum_{k=1}^{\beta} r_k \cdot r_{k+\beta} \\ c_{2,l} &= \sum_{k=1}^{\beta} \tilde{r}_k \cdot r_{k+\beta} \end{aligned} \tag{18}$$

where $\tilde{r}_k$ is the Hilbert transform of the received sequence r_k. Similar to the DCSK system, it is not required to pass the decision variable through thresholding since the output of the correlator is directly connected to the polar decoder.



(**a**) Transmitter (**b**) Receiver

Figure 3. Proposed QCSK transmitter and receiver system.

Figure 4 shows the scheme diagram of the underwater acoustic system (UWAS) employing a differential chaos modulation system. The input data are encoded using a polar coder and then DCSK or QCSK modulation is employed to generate the UWA transmitted signal. At the receiver, the transmitted signal is summed with the noise signal which belongs to a t-distribution, as described in (2) (here, only the noise signal is considered). The received signal under the UWAN channel can be expressed as:

$$r_k = S_k + n_k \tag{19}$$

where n_k is the noise signal that follows a t-distribution with zero mean and variance $N_0/2$. After that, differential chaos demodulation is employed with a soft output and applied to the polar decoder to recover the original data bits.

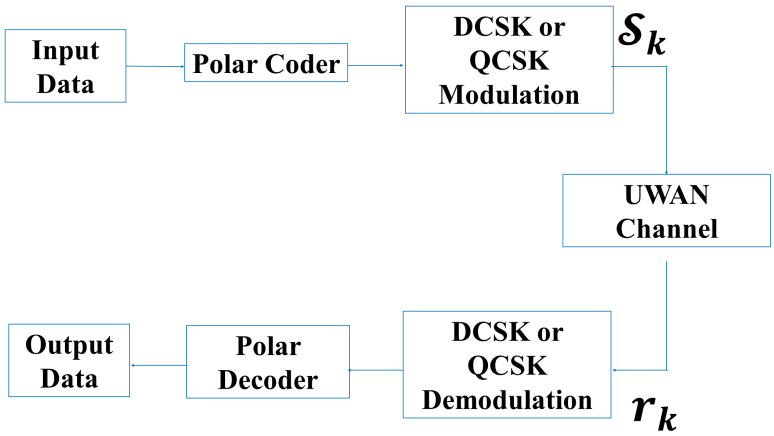


Figure 4. UWAS based on differential chaos modulation.

5. BER Analysis of DCSK and QCSK Systems under the UWA Channel

In this section, the BER formulas of DCSK and QCSK systems for the UWA model are derived using the noise distribution in Section 3. For the DCSK system, after substituting (15) and (19) in (16) and assuming $b_l = +1$, the output of the correlator represented by c_l can be rewritten as:

$$\begin{aligned} c_l &= \sum_{k=1}^{\beta} (x_k + n_k) \cdot (x_k + n_{k+\beta}) \\ &= \sum_{k=1}^{\beta} x_k^2 + 2\sum_{k=1}^{\beta} n_k \cdot x_k + \sum_{k=1}^{\beta} n_k \cdot n_{k+\beta} \end{aligned} \tag{20}$$

The mean μ_1 and the variance σ_1^2 values of c_l are calculated using

$$\mu_1 = E(c_l) = \beta E(x_k^2) \tag{21}$$

$$\sigma_1^2 = V(c_l) = 2\beta \cdot E(x_k^2)\frac{N_0}{2} + \frac{1}{4}\beta \cdot N_0^2 \tag{22}$$

where $E(\cdot)$ is the mean operator and $V(\cdot)$ is the variance operator. Since $E_b = 2\sum x_k^2 = 2\beta E(x_k^2)$, then the mean and variance values in terms of E_b can be expressed as:

$$\begin{aligned} \mu_1 &= E_b/2, \\ \sigma_1^2 &= E_b \cdot \frac{N_0}{2} + \frac{1}{4}\beta \cdot N_0^2 \end{aligned} \tag{23}$$

Similarly, for the QCSK, and by assuming a_l,$b_l = +1$, the decision variable $c_{1,l}$ in (18) is rewritten in terms of (17) and (19) as

$$\begin{aligned} c_{1,l} &= \sum_{k=1}^{\beta}(x_k + n_k)\left(\frac{1}{\sqrt{2}}(x_k + \tilde{x}_k) + n_{k+\beta}\right) \\ &= \frac{1}{\sqrt{2}}\sum_{k=1}^{\beta} x_k^2 + \frac{1}{\sqrt{2}}\sum_{k=1}^{\beta} x_k\tilde{x}_k + \sum_{k=1}^{\beta} x_k n_{k+\beta} + \frac{1}{\sqrt{2}}\sum_{k=1}^{\beta} n_k x_k + \frac{1}{\sqrt{2}}\sum_{k=1}^{\beta} n_k\tilde{x}_k + \sum_{k=1}^{\beta} n_k n_{k+\beta} \end{aligned} \tag{24}$$

By orthogonality, the second term in (24) is zero ($\frac{1}{\sqrt{2}}\sum_{k=1}^{\beta} x_k\tilde{x}_k \approx 0$). The mean, μ_2, and variance, σ_2^2, values of $c_{1,l}$ are expressed as:

$$\mu_2 = E(c_{1,l}) = \frac{1}{\sqrt{2}}\beta E(x_k^2) \tag{25}$$

$$\sigma_2^2 = V(c_{1,l}) = 2\beta \cdot E(x_k^2)\frac{N_0}{2} + \frac{1}{4}\beta \cdot N_0^2 \tag{26}$$

Equations (25) and (26) are rewritten in terms of $E_b = \sum_{k=1}^{\beta} x_k^2 = \beta E(x_k^2)$ as

$$\begin{aligned} \mu_2 &= E_b/\sqrt{2} \\ \sigma_2^2 &= E_b \cdot N_0 + \frac{1}{4}\beta \cdot N_0^2 \end{aligned} \tag{27}$$

Equation (27) is valid for the decision variable $c_{2,l}$. From (23) and (14), the BER formula of the DCSK system can be derived for both degrees of freedom such that

$$\begin{aligned} P_e^5 &= \int_0^{\infty} \frac{0.49}{\sigma}\left(1 + \frac{(x+\mu)^2}{3\sigma^2}\right)^{-3} dx \\ &= 0.5 - \frac{0.55125\sigma\mu(\mu^2 + 5\sigma^2)}{(\mu^2 + 3\sigma^2)^2} - 0.318264\tan^{-1}\left(\frac{\mu}{\sqrt{3}\sigma}\right) \end{aligned} \tag{28}$$

$$\begin{aligned} P_e^6 &= \int_0^{\infty} \frac{0.46875}{\sigma}\left(1 + \frac{(x+\mu)^2}{3\sigma^2}\right)^{-3.5} dx \\ &= 0.5 - \frac{0.015625\mu(\mu^4 + 10\mu^2\sigma^2 + 30\sigma^4)}{(0.25\mu^2 + \sigma^2)^{2.5}} \end{aligned} \tag{29}$$

Similarly, for the QCSK, the BER formula can be written as

$$\begin{aligned} P_e^5 &= 1 - \frac{1.1025\sigma\mu(\mu^2 + 5\sigma^2)}{(\mu^2 + 3\sigma^2)^2} - 0.6365\tan^{-1}\left(\frac{\mu}{\sqrt{3}\sigma}\right) \\ P_e^6 &= 1 - \frac{0.03125\mu(\mu^4 + 10\mu^2\sigma^2 + 30\sigma^4)}{(0.25\mu^2 + \sigma^2)^{2.5}} \end{aligned} \tag{30}$$

6. Simulation and Results

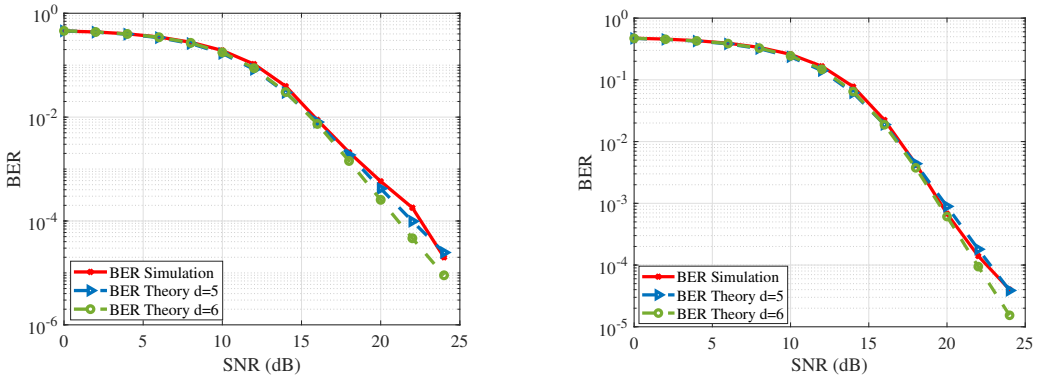
In this section, simulations of the proposed system along with the theoretical results will be presented utilizing MATLAB 2023. Then, the results will be discussed in the next section to demonstrate the performance accuracy.

7. Discussion

Based on the derived BER in Section 5, the simulation in Figure 5 shows the performance of DCSK systems with beta values of 128 and 256. The results show a close match to the derived BER from Equations (28) and (29), which proves that the proposed PDF and the theoretical BER can be used to describe the performance.

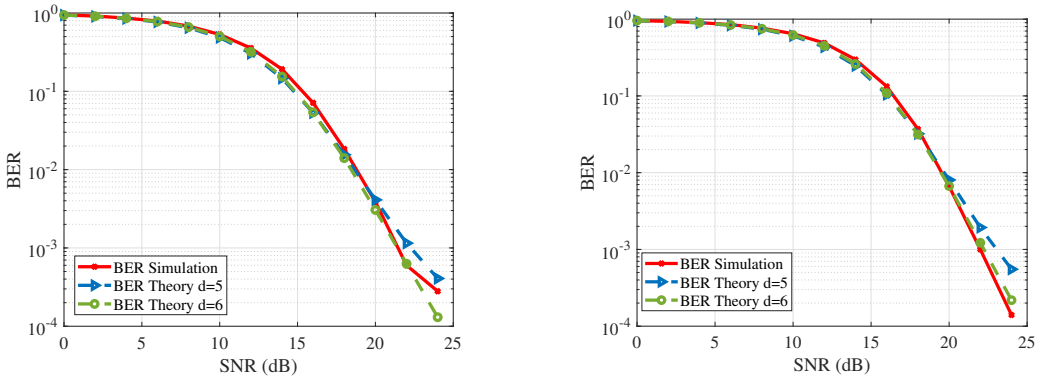
Similarly, Figure 6 demonstrates how well QCSK systems perform with beta values of 128 and 256. The outcomes demonstrate a strong agreement with the derived BER from Equation (30), proving the applicability of both the theoretical BER and the suggested PDF in characterizing the performance.

The outcome displayed in Figures 7 and 8 shows the polar-coded DCSK and QCSK systems' performance for various beta values and for different rates. Depending on the suggested coding rates, the improvement in the performance between the highest and the lowest rates was more than 5 dB for both modulations. In addition, comparing the results of the coded system and the uncoded systems illustrates the polar codes' ability to achieve performance improvements of more than 8 dB in the SNR at the lowest coding rate and 14 dB at the highest rate at BER = 10^{-3}, which can be a challenge in these types of channels.



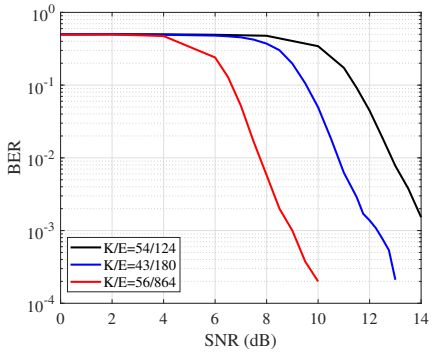
(**a**) DCSK with $\beta = 128$ (**b**) DCSK with $\beta = 256$

Figure 5. DCSK performance with a t−distributed underwater channel compared to Equations (28) and (29) for β = 128 and 256.

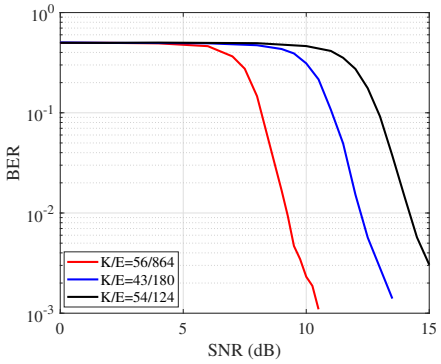


(**a**) QCSK with $\beta = 128$ (**b**) QCSK with $\beta = 256$

Figure 6. QCSK performance with a t−distributed underwater channel compared to Equation (30) for β = 128 and 256.

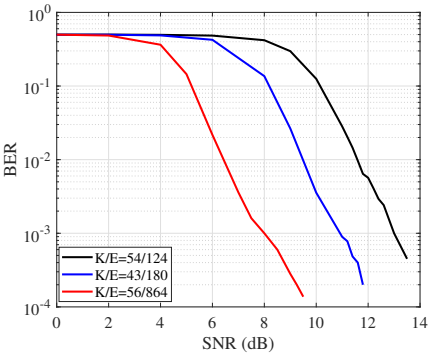


(**a**) Polar-Coded DCSK with $\beta = 128$

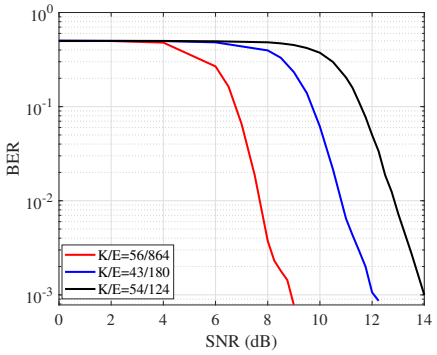


(**b**) Polar-Coded DCSK with $\beta = 256$

Figure 7. Polar-coded DCSK performance with a t−distributed underwater channel and for β = 128 and 256.



(**a**) Polar-Coded QCSK with $\beta = 128$



(**b**) Polar-Coded QCSK with $\beta = 256$

Figure 8. Polar-coded QCSK performance with a t−distributed underwater channel and for β = 128 and 256.

8. Conclusions

In this paper, polar-coded DCSK and polar-coded QCSK in underwater noisy channels are analyzed and simulated. The BER formulas for DCSK and QCSK systems in a UWA noise channel are derived and compared with the simulation results. The experimental results prove that the nearest model that is applicable to the UWA noise channel is the t-distribution with five and six degrees of freedom. In addition, combining polar code with the DCSK system has the ability to achieve performance improvements of about 8, 11 and 14 dB in the SNR at BER = 10^{-3} for coding rates of 0.435, 0.239 and 0.065, respectively, which can be a challenge in UWA noise channels.

Author Contributions: Conceptualization, A.J.A.-A. and F.S.H.; methodology, A.J.A.-A. and F.S.H.; software, A.J.A.-A. and F.S.H.; validation, Y.A.Y., A.J.A.-A. and F.S.H.; formal analysis, A.J.A.-A. and F.S.H.; investigation, Y.A.Y.; resources, Y.A.Y.; data curation, A.J.A.-A. and F.S.H.; writing—original draft preparation, Y.A.Y., A.J.A.-A. and F.S.H.; writing—review and editing, A.J.A.-A. and F.S.H.; visualization, A.J.A.-A. and F.S.H.; supervision, F.S.H.; project administration, Y.A.Y.; funding acquisition, Y.A.Y., A.J.A.-A. and F.S.H. All authors have read and agreed to the published version of the manuscript.

Funding: This research received no external funding.

Data Availability Statement: Data will be made available on request.

Conflicts of Interest: The authors declare no conflict of interest.

Abbreviations

The following abbreviations are used in this manuscript:

UWA	Underwater acoustic
SNR	Signal-to-noise ratio
BER	Bit error rate
DCSK	Differential chaos shift keying
QCSK	Quadrature chaos shift keying
PDF	Probability density function

References

1. Sha'ameri, A.Z.; Al-Aboosi, Y.Y.; Khamis, N.H. Underwater acoustic noise characteristics of shallow water in Tropical Seas. In Proceedings of the International Conference on Computer and Communication Engineering, Kuala Lumpur, Malaysia, 23–25 September 2014. [CrossRef]
2. Chen, P.; Rong, Y.; Nordholm, S.; He, Z.; Duncan, A.J. Joint channel estimation and impulsive noise mitigation in underwater acoustic OFDM communication systems. *IEEE Trans. Wirel. Commun.* **2017**, *16*, 6165–6178. [CrossRef]
3. Chitre, M.; Ong, S.H.; Potter, J. Performance of coded OFDM in very shallow water channels and snapping shrimp noise. In Proceedings of the OCEANS 2005 MTS/IEEE, Washington, DC, USA, 17–23 September 2005. [CrossRef]
4. Ahmed, M.S.; Shah, N.S.M.; Ghawbar, F.; Jawhar, Y.A.; Almohammedi, A.A. Filtered-OFDM with channel coding based on T-distribution noise for underwater acoustic communication. *J. Ambient. Intell. Humaniz. Comput.* **2020**, *13*, 3379–3392. [CrossRef]
5. Li, D.; Wu, Y.; Zhu, M. Nonbinary LDPC code for noncoherent underwater acoustic communication under non-Gaussian noise. In Proceedings of the 2017 IEEE International Conference on Signal Processing, Xiamen, China, 22–25 October 2017. [CrossRef]
6. Yousif Al-Aboosi, Y.; Zuri Sha'ameri, A. Improved underwater signal detection using efficient time–frequency de-noising technique and pre-whitening filter. *Appl. Acoust.* **2017**, *123*, 93–106. [CrossRef]
7. Panaro, J.; Lopes, F.; Barreira, L.; Souza, F. Underwater acoustic noise model for shallow water communications. In Proceedings of the Brazilian telecommunication symposium, Brasilia, Brazil, 13–16 September 2012. [CrossRef]
8. Mohd Shah, N.S.; Al-Aboosi, Y.Y.; Ahmed, M.S. Error performance analysis in underwater acoustic noise with non-Gaussian distribution. *Telecommun. Comput. Electron. Control* **2018**, *16*, 681. [CrossRef]
9. Qarabaqi, P.; Stojanovic, M. Statistical characterization and computationally efficient modeling of a class of underwater acoustic communication channels. *IEEE J. Ocean. Eng.* **2013**, *38*, 701–717. [CrossRef]
10. Ren, H.-P.; Kong, Q.-J.; Bai, C. A chaotic spread spectrum system for underwater acoustic communication. In Proceedings of the 2015 IEEE International Wireless Symposium, Shenzhen, China, 30 March–1 April 2015. [CrossRef]
11. Chen, M.; Xu, W.; Wang, D.; Wang, L. Statistical Multi-carrier chaotic communication scheme for underwater acoustic communications. *IET Commun.* **2019**, *13*, 2097–2105. [CrossRef]
12. Morozs, N.; Gorma, W.; Henson, B.T.; Shen, L.; Mitchell, P.D.; Zakharov, Y.V. Channel modeling for underwater acoustic network simulation. *IEEE Access* **2020**, *8*, 136151–136175. [CrossRef]
13. Zanaj, E.; Gambi, E.; Zanaj, B.; Disha, D.; Kola, N. Underwater wireless sensor networks: Estimation of acoustic channel in shallow water. *Appl. Sci.* **2020**, *18*, 6393. [CrossRef]
14. Chen, Y.; Yu, W.; Sun, X.; Wan, L.; Tao, Y.; Xu, X. Environment-aware communication channel quality prediction for underwater acoustic transmissions: A machine learning method. *Appl. Acoust.* **2021**, *181*, 108–128. [CrossRef]
15. Wang, S.; He, Z.; Niu, K.; Chen, P.; Rong, Y. New results on joint channel and impulsive noise estimation and tracking in underwater acoustic OFDM systems. *IEEE Trans. Wirel. Commun.* **2020**, *19*, 2601–2612. [CrossRef]
16. Wei, Y.; Quan, L.; Xu, W.; Wang, D.; Wang, L. An in-phase/quadrature index modulation-aided spread spectrum communication system for underwater acoustic communication. *Electronics* **2023**, *12*, 2919. [CrossRef]
17. Arikan, E. Channel Polarization: A method for constructing capacity-achieving codes for symmetric binary-input memoryless channels. *IEEE Trans. Inf. Theory* **2009**, *55*, 3051–3073. [CrossRef]
18. Coladarci, T.; Cobb, C.D.; Minium, E.W.; Clarke, R.C. *Fundamentals of Statistical Reasoning in Education*; John Wiley & Sons: New York, NY, USA, 2010.
19. Al-Askery, A.J.; Tsimenidis, C.C.; Boussakta, S.; Chambers, J.A. Performance analysis of coded massive MIMO-OFDM systems using effective matrix inversion. *IEEE Trans. Commun.* **2017**, *65*, 5244–5256. [CrossRef]
20. Al-Askery, A.; Al-Naji, A.; Alsabah, M. Improving the performance of turbo-coded systems under Suzuki fading channels. *J. Low Power Electron. Appl.* **2019**, *9*, 13. [CrossRef]

21. Xia, Y.; Tse, C.K.; Lau, F.C.M. Performance of differential chaos-shift-keying digital communication systems over a multipath fading channel with delay spread. *IEEE Trans. Circuits Syst. II Express Briefs* **2004**, *51*, 680–684. [CrossRef]
22. Galias, Z.; Maggio, G.M. Quadrature chaos-shift keying: Theory and performance analysis. *IEEE Trans. Circuits Syst. Fundam. Theory Appl.* **2001**, *48*, 1510–1519. [CrossRef]

Disclaimer/Publisher's Note: The statements, opinions and data contained in all publications are solely those of the individual author(s) and contributor(s) and not of MDPI and/or the editor(s). MDPI and/or the editor(s) disclaim responsibility for any injury to people or property resulting from any ideas, methods, instructions or products referred to in the content.